JTTEE5 6:353-360

Flattening of Composite Powder Particles during Thermal Spraying

V.V. Sobolev, J.M. Guilemany, and A.J. Martín

An investigation is conducted of the time evolution of the splat thickness, radius, and rate characteristics in the process of flattening of composites (agglomerated) powder particles at smooth and rough surfaces during thermal spraying. Considerations include the splat solidification, droplet mass loss, solid volume fraction, and variations of splat-surface friction and splat solidification velocity due to the presence of the solid phase. Effective values of the droplet viscosity, impact velocity, and Reynolds number taking into account characteristic features of the flattening process are introduced, and analytical formulas describing the final values of the splat thickness, radius, and rate characteristics are established. Results can be used to predict the splat flattening parameters.

Keywords composite particle, flattening, solid phase, splat-surface friction, thermal spraying, volume fraction

1. Introduction

Composite powders consisting of a solid phase (carbides, oxides, etc.) and a metallic binder (nickel, chromium, cobalt, etc.) play an important role in the development of thermally sprayed coatings with increased wear and corrosion resistance (Ref 1). The structure and properties of these coatings depend essentially on the dynamics of flattening of the melted particles (droplets) of composite powders on a substrate surface.

The dynamics of the droplet flattening upon impact have been studied experimentally and theoretically in a number of papers, which are reviewed in Ref 2 and in more recent publications (Ref 3-9). The results obtained enable prediction of the splat dimensions, which significantly influence its further cooling and solidification (Ref 10-13).

This article investigates the flattening dynamics of composite powder particles during thermal spraying and presents analytical formulas that permit estimation of this process during practice. These formulas consider the roughness of the substrate surface, the splat solidification, and mass loss due to splashing and crater formation in the surface where the flattening occurs.

2. General Ideas

Consider an agglomerate composite particle consisting of small, high-melting-point solid components (e.g., carbides) and a binding metal. Assume that during thermal spraying the binder melts and this particle of radius R_P impinges normally with a velocity U onto the surface of a substrate or previously deposited coating layer and forms a cylindrical splat of radius R and thickness b, which vary with time (t) during flattening. Assume further that the solid components are markedly smaller than the splat thickness and that the surface roughness ε_0 and a liquid-solid mixture of the impinging droplet can be considered as a quasi-homogeneous medium with a solid volume fraction φ.

Since there is no great difference between the densities of liquid and solid phases of the droplet, it is reasonable to assume that the relative movement between these phases is negligible in the bulk volume of the splat and, therefore, the interaction forces between them can be neglected (Ref 14). With the small value of φ, the liquid-solid mixture of the droplet can be considered as a uniform medium with the effective dynamic viscosity μ_* (Ref 15):

$$\mu_* = \mu(1 - \varphi)^{-1} \quad \text{(Eq 1)}$$

where μ is the dynamic viscosity of the liquid phase.

Equation 1 shows that the presence of the solid phase increases the flow viscosity. This occurs also due to the non-Newtonian character of the liquid-solid flow, which becomes more pronounced under temperatures near the solidification point (Ref 15, 16). During flattening the spreading flow is turbulent, and at the droplet/substrate interface friction decreases in comparison with a single-phase flow because of reduced mixing length due to dissipation by the solid particles (Ref 15).

To take into account the roughness, ε, of the substrate surface during the flattening process, assume that it increases the shear stress by the value that arises because of friction between a flattening droplet and the rough surface. In accordance with Ref 6, we use the modified Blench formula for the friction coefficient, f, with a correction factor, ω, accounting for a decrease in friction in the liquid-solid flow:

$$f = 0.79\,\omega\sqrt{\frac{\varepsilon}{R_P}} = 0.79\omega\sqrt{\alpha} \quad \text{(Eq 2)}$$

In the case of the smooth surface, the friction coefficient can be described by this correlation (Ref 9):

$$f = 0.664\,\omega Re_*^{-1/2}$$

$$Re_* = \frac{2R_P U\rho}{\mu_*} \quad \text{(Eq 3)}$$

where Re_* is the characteristic Reynolds number and ρ is the density of the liquid phase. When $\omega = 1$ and $\varphi = 0$, from Eq 2 and 3 we obtain the formulas used in Ref 6 and 9.

V.V. Sobolev, J.M. Guilemany, and **A.J. Martín,** Metalurgia Física-Ciencia de Materiales, Centro de Proyección Térmica, Departamento de Ingeniería Química y Metalurgia, Universidad de Barcelona, Martí i Franqués, 1, 08028 Barcelona, Spain.

The main heat removal from the splat takes place from its lower part due to the substrate heat sink (Ref 10, 12). The solidification front moves from the surface of the substrate or the surface of the already deposited coating layer with a velocity of V_S inside the splat. It gradually decreases the surface roughness and will cover it completely at the time of $t_S = \varepsilon_0 V_S^{-1}$. The ratio, η, of the impact time $R_P U^{-1}$ to t_S gives the degree of the influence of the splat solidification on the part of the flattening process associated with the surface roughness (Ref 8):

$$\eta = \frac{R_P V_S}{\varepsilon_0 U} \quad \text{(Eq 4)}$$

Also consider that roughness, ε, is changed during splat solidification according to a formula that is valid when $t < \varepsilon_0 V_S^{-1}$ (Ref 6):

$$\varepsilon = \varepsilon_0 - V_S t \quad \text{(Eq 5)}$$

The liquid-solid splat solidification velocity depends on the thermophysical properties of the liquid and solid phases and the contact heat-transfer coefficient α_C at the splat/substrate interface. If the thermal diffusivity of solid (e.g., tungsten carbide) a_S is greater than that of liquid a_L (metallic binder), this contributes to an increase in the rate of heat transfer inside the splat. However, an increase in V_S would hardly ever occur because of the relatively large contact thermal resistance at the interface (Ref 2).

The most important case is when the thermal diffusivity of the solid (e.g., oxide) is less than that of the liquid phase. Then the heat-transfer rate inside the splat decreases. This decrease can be more pronounced when the solid density ρ_S exceeds that of the liquid phase and solid particles precipitate in the lower part of the splat. The surface roughness introduces a certain nonuniformity to precipitation because the solid particles can be precipitated in the wavy structure of the rough surface.

The characteristic time of precipitation, t_P, can be estimated as bU^{-1}. Roughness will be important during precipitation of solids if it is not covered by the solidification front moving with the velocity V_S. This front will cover the surface roughness completely at the time t_S. Therefore, the degree of roughness influence on the precipitation process is determined by the ratio, κ, of the time t_P to t_S.

$$\kappa = \frac{bV_S}{\varepsilon_0 U} \quad \text{(Eq 6)}$$

Since the splat thickness, b, is of the same order of magnitude as the initial surface roughness, ε_0, and the droplet impinging velocity, U, is much greater than V_S, the value $\kappa << 1$ for thermal spray processes. Thus, surface roughness plays an important role in the precipitation of solids.

When $a_S < a_L$ and $\rho_S > \rho_L$, the precipitation of solids can lead to an increase in the contact thermal resistance, R_C, at the interface. This occurs if the thermal resistance, R_{CP}, of the precipitate layer of solid is greater than that, R_{CO}, at the interface when the solid surface is absent ($\varphi = 0$) or is comparable to R_{CO}.

Consider an example of high-velocity oxyfuel (HVOF) spraying of Cr_3C_2-NiCr powder onto a steel substrate. An impinging molten droplet consists of the solid phase, including different chromium carbides and chromium oxide (Cr_2O_3), and the liquid phase, including an alloy Cr-Ni-C formed due to in-flight dissolution of Cr_3C_2 (Ref 17). For the contact thermal resistance the most critical is precipitation of chromium oxide, which has a low thermal conductivity, λ_1.

The thermal resistance, R_1, of the layer of Cr_2O_3 with a thickness of δ_1 is equal to $\delta_1 \lambda_1^{-1}$. Assume that the rough substrate surface consists of rectangular "teeth" with an initial height of ε_0. Their length is assumed to be equal to the distance between them. To estimate R_1, let the value of δ_1 be equal to 0.5 ε_0. When $\delta_1 = 2$ μm and $\lambda_1 = 20$ W/m · K, we have $R_1 = 10^{-7}$ m²K/W.

Symbols

R_P	Particle radius, m
U	Particle (droplet) impact velocity, m/s
R	Splat radius, m
b	Splat thickness, m
t	Time, s
f	Friction coefficient
V_S	Solidification velocity, m/s
t_S	Characteristic time, s: $t_S = \varepsilon_0 V_S^{-1}$
a_S	Solid-phase thermal diffusivity, m²/s
a_L	Liquid-phase thermal diffusivity, m²/s
t_P	Characteristic time, s: $t_P = bU^{-1}$
R_C	Contact thermal resistance, m²K/W
R_{CP}	Contact thermal resistance of the precipitate layer, m²K/W
R_{CO}	Contact thermal resistance at the interface, m²K/W
R_1	Layer thermal resistance, m²K/W
T	Splat temperature, °C
Re	Reynolds number

Greek Symbols

ε	Roughness in size, m
φ	Solid volume fraction
μ	Droplet dynamic viscosity, N · s/m²
η	Dimensionless parameter: $\eta = R_P V_S/(\varepsilon_0 U)$
α_C	Contact heat-transfer coefficient, W/m² · K
ρ	Droplet density, kg/m³
ρ_L	Liquid-phase density, kg/m³
ρ_S	Solid-phase density, kg/m³
κ	Dimensionless parameter: $\kappa = bV_S/(\varepsilon_0 U)$
δ_1	Layer thickness, m
λ_1	Layer thermal conductivity, W/m · K
ω, ψ	Correction factor
ζ	Dimensionless splat thickness: $\zeta = b/R_P$
ξ	Dimensionless splat radius: $\xi = R/R_P$
θ	Dimensionless time: $\theta = UR_P^{-1}t$
γ	$\gamma = \exp(0.4\theta)$
χ	Dimensionless parameter of droplet mass loss

Subscripts

0	Initial
*	Characteristic
e	Effective
f	Final

This value of R_1 can be comparable to R_{CO} and even exceed it (Ref 18). This indicates that in this case the presence of the solid phase in the splat leads to an increase in the contact thermal resistance at the splat/substrate interface and thus to a decrease in the solidification velocity, V_S.

The solidification velocity can be calculated by methods described elsewhere (Ref 10, 12) or measured experimentally (Ref 18). It can also be estimated by (Ref 8):

$$V_S = \frac{\alpha_C T}{q\rho} \quad \text{(Eq 7)}$$

where T is the splat temperature and q is the latent heat of fusion of the liquid phase.

To take into account the solidification process during flattening of the composite droplets, it is worth introducing the solidification velocity, V_{S*}, with a correction factor, ψ, which accounts for the changes in V_S associated with the solid phase of the droplet:

$$V_{S*} = \psi V_S \quad \text{(Eq 8)}$$

The most probable situation corresponds to $\psi < 1$.

It also is convenient to introduce the dimensionless variables:

$$\xi = \frac{R}{R_P}$$

$$\zeta = \frac{b}{R_P}$$

$$\beta_* = \frac{V_{S*}}{U}$$

$$\theta = UR_P^{-1}t \quad \text{(Eq 9)}$$

3. Analytical Formulas

3.1 *Transient Characteristics of Flattening*

Consider first the flattening of an impinging droplet on a smooth surface. Using the equations and methods described in Ref 5, 8, and 9, and Eq 1, 3, and 8, the following expressions are obtained for the dimensionless splat thickness, ζ; the splat radius, ξ; and the rate characteristics of the flattening process, $d\zeta/d\theta$ and $d\xi/d\theta$ when $Re_* >> 1$:

$$\zeta = \gamma^{-1}\,[1 + 0.15\omega Re_*^{-1/2}(\gamma - 1) - \beta_*\theta\gamma],\ \gamma = \exp(0.4\theta) \quad \text{(Eq 10)}$$

$$\xi = 1.155\sqrt{\chi\gamma}\,[1 - 0.075\,\omega Re_*^{-1/2}(\gamma - 1) + 0.5\beta_*\theta\gamma] \quad \text{(Eq 11)}$$

$$\frac{d\zeta}{d\theta} = -0.4\gamma^{-1}\,[1 - 0.15\,\omega Re_*^{-1/2} + 2.5\beta_*\gamma] \quad \text{(Eq 12)}$$

$$\frac{d\xi}{d\theta} = 0.231\sqrt{\chi\gamma}\,[1 - 0.075\,\omega Re_*^{-1/2}(3\gamma - 1) + 2.5\beta_*\gamma + 1.5\beta_*\theta\gamma] \quad \text{(Eq 13)}$$

where χ is the ratio of the droplet mass that remains after the losses in mass of an impinging droplet during impact (due to splashing and crater formation in the surface) to the initial mass of the impinging droplet.

When $\varphi = 0$, $\omega = 1$, $\psi = 1$ from Eq 10 to 13, we have the formulas obtained in Ref 8 and 9. From Eq 10 to 13 it follows that an increase in the solid volume fraction φ, which leads to a decrease in the Reynolds number Re_*, causes a decrease in the splat thickness ζ and an increase in the splat radius ξ, the rate parameter $d\xi/d\theta$, and the absolute value of $d\zeta/d\theta$. Since $\omega < 1$, the presence of the solid phase in the splat contributes to the above events. A decrease in the solidification velocity in the liquid-solid mixture ($\psi < 1$ and $V_{S*} < V_S$) gives rise to ζ and decreases ξ, $|d\zeta/d\theta|$, and $d\xi/d\theta$.

Consider now the flattening of the impinging droplet on a rough surface. Using the equations and methods given in Ref 5, 6, and 8, and Eq 1, 2, 4, and 8, the following expressions are obtained for ζ, ξ, $d\zeta/d\theta$, and $d\xi/d\theta$ when $Re_* >> 1$:

$$\zeta = \gamma^{-1}[1 + 0.22\,\omega\sqrt{\alpha}(\gamma - 1) - \beta_*\theta\gamma]$$

$$\alpha = \alpha_0 - \beta_*\theta \quad \text{(Eq 14)}$$

$$\xi = 1.155\sqrt{\chi\gamma}\,[1 - 0.11\,\omega\sqrt{\alpha}(\gamma - 1) + 0.5\beta_*\theta\gamma] \quad \text{(Eq 15)}$$

$$\frac{d\zeta}{d\theta} = -0.4\gamma^{-1}[1 - 0.22\,\omega\sqrt{\alpha} + 0.275\,\eta_*\omega\sqrt{\alpha}(\gamma - 1) + 2.5\beta_*\gamma]$$

$$\eta_* = R_P V_{S*}(\varepsilon_0 U)^{-1} \quad \text{(Eq 16)}$$

$$\frac{d\xi}{d\theta} = 0.231\sqrt{\chi\gamma}\,[1 - 0.11\,\omega\sqrt{\alpha}(3\gamma - 1) + 0.275\,\eta_*\omega\sqrt{\alpha}(\gamma - 1) + 2.5\beta_*\gamma + 1.5\beta_*\theta\gamma] \quad \text{(Eq 17)}$$

When $\varphi = 0$, $\omega = 1$, and $\psi = 1$ from Eq 14 to 17, we have the formulas obtained in Ref 6 and 8. Comparison of Eq 10 to 13 with Eq 14 to 17 shows that the influence of parameters φ, ω, and ψ on the liquid-solid droplet flattening at the rough surface is qualitatively the same as in the case of the droplet flattening at the smooth surface with the droplet/surface friction.

3.2 *Final Characteristics of Flattening*

Considering the droplet flattening on the smooth surface and using the equations and methods described in Ref 5, 8, and 9, we obtain the following formulas for the final flattening parameters ζ_f, ξ_f, $d\zeta_f/d\theta$, and $d\xi_f/d\theta$:

$$\zeta_f = 1.826\, Re_*^{-1/2}\,[1 + 0.15\,\omega Re_*^{-1/2}(0.55\, Re_*^{1/2} - 1) - 0.68\,\beta_* Re_*^{1/2} \ln(1 + 0.3\, Re_*)] \quad \text{(Eq 18)}$$

$$\xi_f = 0.8546\,\sqrt{\chi}\, Re_*^{1/4}\,[1 - 0.075\,\omega Re_*^{-1/2}(0.55\, Re_*^{1/2} - 1) + 0.34\,\beta_* Re^{1/2} \ln(1 + 0.3\, Re_*)] \quad \text{(Eq 19)}$$

$$\frac{d\zeta_f}{d\theta} = -0.73\, Re_*^{-1/2}\,[1 - 0.15\,\omega Re_*^{-1/2} + 1.37\,\beta_* Re_*^{1/2}] \quad \text{(Eq 20)}$$

$$\frac{d\xi}{d\theta} = 0.171\,\sqrt{\chi}\, Re_*^{1/4}\,[1 - 0.075\,\omega Re_*^{-1/2}(1.65\, Re_*^{1/2} - 1) + 1.37\,\beta_* Re_*^{1/2} + 1.03\,\beta_* Re_*^{1/2} \ln(1 + 0.3\, Re_*)] \quad \text{(Eq 21)}$$

With very high values of Re_*, the rate parameter $d\zeta_f/d\theta$ remains the same, and with $\omega < 1$ from Eq 18, 19, and 21 it follows that the maximum contributions of the splat/surface friction to the final values of ζ_f, ξ_f, and $d\xi_f/d\theta$ are about 8, 4, and 12%, respectively. Thus, when $Re_* >> 1$, the friction effects can be neglected. Then the final values of ζ_f, ξ_f, and $d\xi_f/d\theta$ are as follows:

$$\zeta_f = 1.826\, Re_*^{-1/2}\,[1 - 0.68\,\beta_* Re_*^{1/2} \ln(0.3\, Re_*)] \quad \text{(Eq 22)}$$

$$\xi_f = 0.8546\,\sqrt{\chi}\, Re_*^{1/4}\,[1 + 0.34\,\beta_* Re_*^{1/2} \ln(0.3\, Re_*)] \quad \text{(Eq 23)}$$

$$\frac{d\xi_f}{d\theta} = 0.171\,\sqrt{\chi}\, Re^{1/4}\,[1 + 1.37\,\beta_* Re_*^{1/2} + 1.03\,\beta_* Re_*^{1/2} \ln(0.3\, Re_*)] \quad \text{(Eq 24)}$$

When $\varphi = 0$, $\omega = 1$, and $\psi = 1$ from Eq 22 to 24, we have the formulas describing the influence of the splat solidification on the flattening process (Ref 8, 9). Due to the presence of the solid phase ($\varphi > 0$ and $\psi < 1$), this influence on the final values ζ_f, ξ_f, and $d\xi_f/d\theta$ of the flattening parameters is weaker than in the case of the homogeneous splat.

In the case of the droplet flattening on the rough surface using the results of Ref 6 and 8, the following formulas can be obtained for the flattening characteristics:

$$\zeta_f = 1.826\, Re_*^{-1/2}\,[1 + 0.22\,\omega\sqrt{\alpha}(0.55\, Re_*^{1/2} - 1) - 0.68\,\beta_* Re_*^{1/2} \ln(1 + 0.3\, Re_*)] \quad \text{(Eq 25)}$$

$$\xi_f = 0.8546\,\sqrt{\chi}\, Re_*^{1/4}\,[1 - 0.11\,\omega\sqrt{\alpha}(0.55\, Re_*^{1/2} - 1) + 0.34\,\beta_* Re_*^{1/2} \ln(1 + 0.3\, Re_*)] \quad \text{(Eq 26)}$$

$$\frac{d\zeta_f}{d\theta} = -0.73\, Re_*^{-1/2}[1 - 0.22\,\omega\sqrt{\alpha} + 0.275\,\eta_*\omega\sqrt{\alpha}(0.55\, Re_*^{1/2} - 1) + 1.37\,\beta_* Re_*^{1/2}] \quad \text{(Eq 27)}$$

$$\frac{d\xi_f}{d\theta} = 0.171\,\sqrt{\chi}\, Re_*^{1/4}\,[1 - 0.11\,\omega\sqrt{\alpha}(1.64\, Re_*^{1/2} - 1) + 0.275\,\eta_*\omega\sqrt{\alpha}(0.55\, Re_*^{1/2} - 1) + 1.37\,\beta_* Re_*^{1/2} + 1.03\,\beta_* Re_*^{1/2} \ln(1 + 0.3\, Re_*)] \quad \text{(Eq 28)}$$

Under very high values of Re_* from Eq 25 to 28 we have:

$$\zeta_f = 1.826\, Re_*^{-1/2}\,[1 + 0.12\,\omega\sqrt{\alpha}\, Re_*^{1/2} - 0.68\,\beta_* Re_*^{1/2} \ln(0.3\, Re_*)] \quad \text{(Eq 29)}$$

$$\xi_f = 0.8546\,\sqrt{\chi}\, Re_*^{1/4}\,[1 - 0.06\,\omega\sqrt{\alpha}\, Re_*^{1/2} + 0.34\,\beta_* Re_*^{1/2} \ln(0.3\, Re_*)] \quad \text{(Eq 30)}$$

$$\frac{d\zeta_f}{d\theta} = -0.73\, Re_*^{-1/2}(1 - 0.22\,\omega\sqrt{\alpha} + 0.15\,\eta_*\omega\sqrt{\alpha}\, Re_*^{1/2} + 1.37\,\beta_* Re_*^{1/2}) \quad \text{(Eq 31)}$$

$$\frac{d\xi_f}{d\theta} = 0.171\,\sqrt{\chi}\, Re_*^{1/4}\,[1 - 0.18\,\omega\sqrt{\alpha}\, Re_*^{1/2} + 0.15\,\eta_*\omega\sqrt{\alpha}\, Re_*^{1/2} + 1.37\,\beta_* Re_*^{1/2} + 1.03\,\beta_* Re_*^{1/2} \ln(0.3\, Re_*)] \quad \text{(Eq 32)}$$

When $\varphi = 0$, $\omega = 1$, and $\psi = 1$ from Eq 29 to 32, we obtain the formulas established in Ref 6 and 8. It is seen from Eq 29 to 32 that, without taking into account the surface roughness ($\alpha = 0$) and the splat solidification ($\beta_* = 0$), the presence of the solid particles in the flattening droplet ($\varphi \neq 0$) leads to an increase in the final splat thickness and the final absolute value of $d\zeta_f/d\theta$ and to a decrease in ξ_f and the value of $d\xi_f/d\theta$ in comparison with the homogeneous droplet ($\varphi = 0$). This occurs because of the additional energy dissipation caused by the solid phase.

When $\varphi \neq 0$, the contributions of the surface roughness and the splat solidification to the flattening characteristics are less pronounced than in the case when $\varphi = 0$. Their relative contributions depend on the specific values of φ, ω, and ψ.

Use of the analytical expressions given in Eq 29 and 30 shows that in the absence of the splat solidification ($\beta_* = 0$) the influence of the surface roughness is equivalent to the influence of an effective viscosity, μ_{*e}, which with an accuracy of the order $0(\alpha)$ is as follows:

$$\mu_{*e} = \mu_*(1 + 0.24\,\omega\sqrt{\alpha}\,Re_*^{1/2}) \qquad \text{(Eq 33)}$$

For the flattening at a smooth surface ($\alpha = 0$) without splat/surface friction, the influence of the splat solidification is equivalent to the influence of an effective velocity, U_e, of the droplet impingement. From Eq 29 and 30 it follows that with an accuracy up to the terms of the order $0(\beta^2)$ the value of U_e is as follows:

$$U_e = U\,[1 + 0.34\,\beta_* Re_*^{1/2} \ln (0.3 Re_*)]^4 \qquad \text{(Eq 34)}$$

Using Eq 29 and 30, it can be shown that the liquid-solid droplet flattening at a rough surface with splat solidification is equivalent to the flattening at the smooth surface without splat solidification and with negligible influence of splat/surface friction, under conditions when the velocity of droplet impingement is U_e and the dynamic viscosity of the droplet is μ_{*e}. Under these conditions Eq 29 and 30, with an accuracy up to the terms of the order $0(\alpha, \beta^2)$, can be written as:

$$\zeta_f = 1.826\,Re_{*e}^{-1/2},\ R_{*e} = 2R_p U_e \rho \mu_{*e}^{-1} \qquad \text{(Eq 35)}$$

$$\xi_f = 0.8546\,\sqrt{\chi}\,Re_{*e}^{1/4} \qquad \text{(Eq 36)}$$

When $\varphi = 0$, $\omega = 1$, and $\psi = 1$ from Eq 35 and 36, we have the formulas obtained in Ref 6 to 9.

3.3 *Numerical Simulation*

To examine the transient characteristics of the flattening process, Eq 10 to 13 and Eq 14 to 17 were studied numerically.

In the case of the rough surface, the calculations based on Eq 14 to 17 were performed when $\alpha_0 = 0.2$. Figure 1 shows that the splat thickness decreases with an increase and in β and ψ and a decrease in ω. The splat radius increases when ω decreases and β, ψ, and χ increase (Fig. 2). Figure 3 shows that the absolute value of $d\zeta/d\theta$ increases with a decrease in ω and an increase in β and ψ. The parameter $d\xi/d\theta$ varies nonuniformly with θ when $\psi = 1$, $\omega = 1$, $\chi = 1$, and $\beta = 0$ (Fig. 4, curve 1). The behavior of $d\xi/d\theta$ becomes more uniform with an increase in β and a decrease in ω and ψ, and under these conditions the value of $d\xi/d\theta$ increases with an increase in θ.

In the case of the smooth surface, the results of the numerical analysis of Eq 10 to 13 when $Re = 400$ are shown in Fig. 5 to 7.

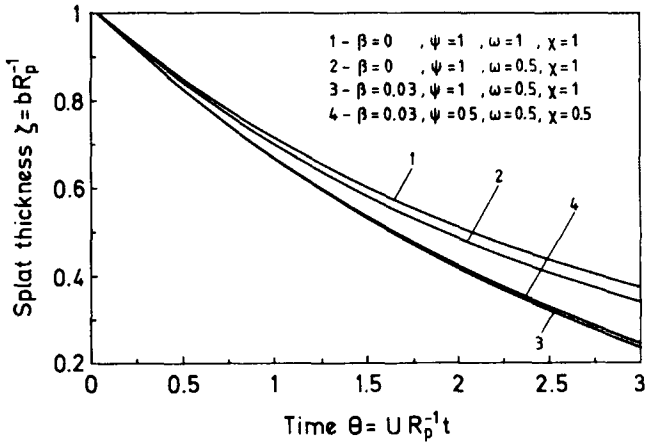

Fig. 1 Variation of splat thickness with time for the rough surface

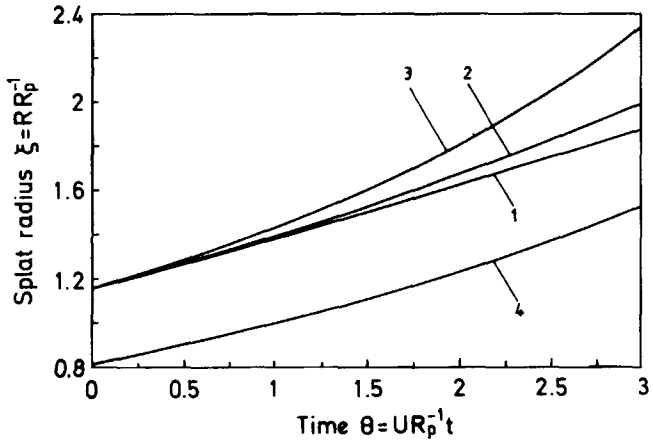

Fig. 2 Variation of the splat radius with time for the rough surface

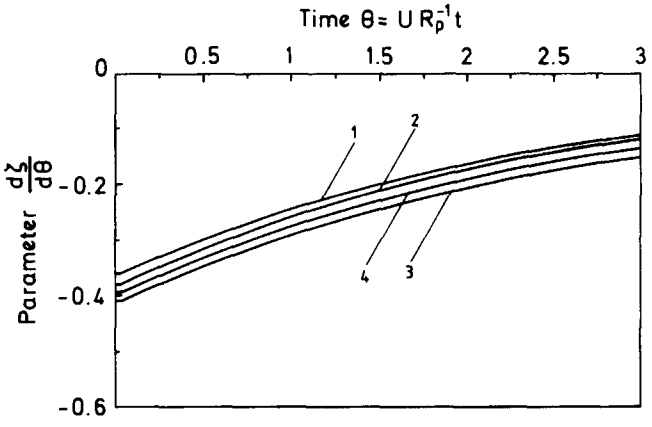

Fig. 3 Variation of the rate parameter $d\zeta/d\theta$ with time for the rough surface

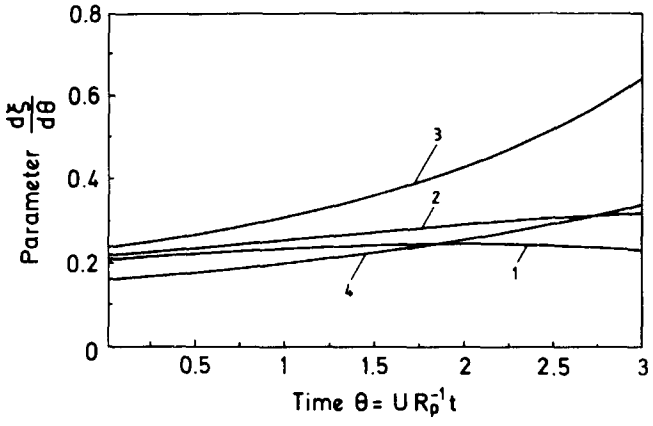

Fig. 4 Variation of the rate parameter $d\xi/d\theta$ with time for the rough surface

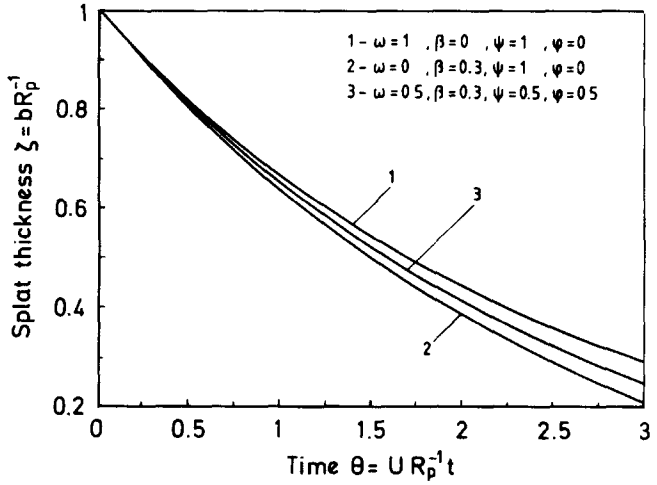

Fig. 5 Variation of splat thickness with time for the smooth surface

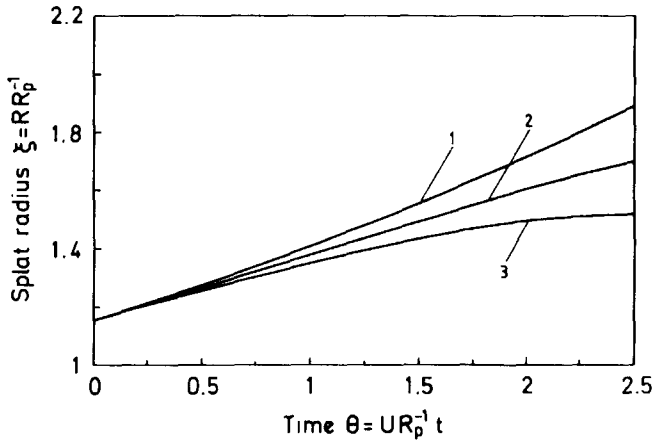

Fig. 6 Variation of the splat radius with time for the smooth surface

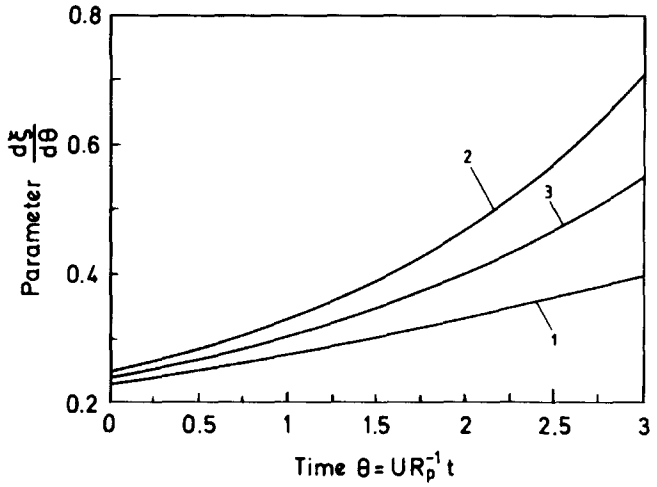

Fig. 7 Variation of the rate parameter $d\xi/d\theta$ with time for the smooth surface

The splat thickness decreases when β increases and ω decreases (Fig. 5). An increase in φ and a decrease in ψ lead to an increase in ζ. Figure 6 shows that the splat radius decreases when φ and ω are increased. A decrease in ψ causes a decrease in ξ. The absolute value of $d\zeta/d\theta$ decreases with an increase in θ and depends weakly on the changes in the spray parameters. The value of $d\xi/d\theta$ enhances with an increase in β and decreases with an increase in ω and φ.

The practice of thermal spraying also requires knowing the variations of the final parameters of flattening. In the case of the rough surface, numerical analysis of Eq 25 and 26 when $\beta = 0.03$ produces the curves shown in Fig. 8 and 9. The final splat thickness decreases with an increase in the Reynolds number (Fig. 8). The value of ζ_f undergoes an increase with an increase in φ and ω. The final splat thickness enhances when ψ decreases. Figure 9 shows that the final splat radius decreases with an increase in φ and ω. The value of ξ_f enhances when χ and ψ increase.

For the smooth surface, Eq 18 and 19 produce curves for the final splat thickness and radius similar to those shown in Fig. 8 and 9. As an example, the variations of ξ_f with *Re* are given in Fig. 10, which shows that the final splat radius increases with a decrease in ω. An increase in χ and ψ leads to an increase in ξ_f. The value of ξ_f decreases when φ increases.

Table 1 Comparison of theoretical and experimental results

Coating type	b, μm	d_P, μm	d_P/b Calculated	d_P/b Experimental
1	2.27 ± 0.95	20	12.89	6.21-15.15
2	2.37 ± 0.95	38	13.07	11.45-26 76
3	2.93 ± 0.95	40	13.10	10.31-20.20

4. Comparison with Experimental Data

The effect of WC particle size on the flattening of WC-Co splats during HVOF spraying was studied experimentally in Ref 19. In this article, four types of WC-Co powders were considered: sintered-crushed (types 1 and 2), agglomerated (type 3), and coated (type 4). We shall compare experimental data for the first three types of WC-Co powders, which correspond to those studied above.

Our calculations will use Eq 25 for the final value, $\zeta_f = bR_P^{-1}$, of the splat thickness and will consider the splat solidification negligible (Ref 19). Take $\rho = 14{,}900$ kg/m^3, $\mu = 3 \times 10^{-3}$ kg · m^{-1} · s^{-1}, $\omega = 0.9$, $\varphi = 0.3$, and $\alpha = 0.5$. For powder type 1, U = 325 m/s; for powder types 2 and 3, U = 190 m/s (Ref 19). Then, for the different values of the particle diameter d_P, the calculated values of the ratio d_P/b are obtained and compared in Table 1 with the corresponding experimental values of d_P/b given in Ref 19. It can be seen that the theoretical results agree well with the experimental data.

5. Conclusions

The approximate equations describing the time evolution of the thermally sprayed splat thickness and radius as well as the

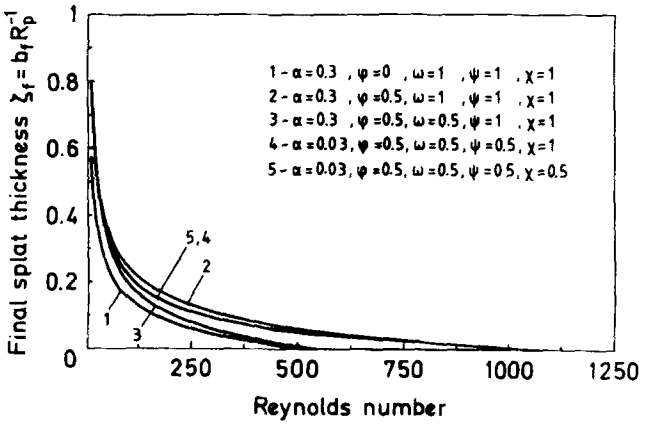

Fig. 8 Variation of final splat thickness with Reynolds number for the rough surface

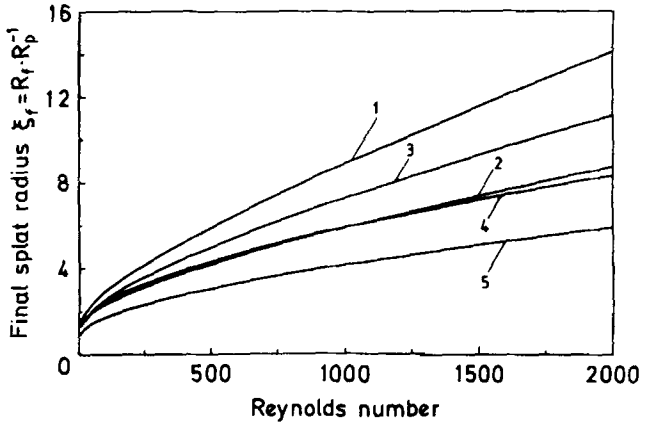

Fig. 9 Variation of final splat radius with Reynolds number for the rough surface

rates of their variation during the flattening of composite powder particles consisting of solid phase and binder are established, taking into account an increase in particle viscosity and a decrease in the friction at the splat/substrate interface and in the velocity of solidification of the lower part of the splat. Realistic correlations between the final values of the splat thickness, splat radius and their variation rates, and the Reynolds number are obtained by taking into account these phenomena.

An effective dynamic viscosity of the splat liquid phase is introduced that accounts for the solid-phase influence on the flow of the solid-liquid mixture during the droplet flattening. In the case of flattening at a rough surface, the splat thickness decreases with time and with an increase in solidification velocity and coefficient ψ. The value of ζ decreases when coefficient ω decreases. The splat radius increases with time and with a decrease in ω and an increase in β, ψ, and χ.

The absolute value of the rate parameter $d\zeta/d\theta$ enhances with a decrease in ω and an increase in β and ψ. The rate parameter $d\xi/d\theta$ varies nonuniformly with time, and its behavior becomes more uniform when β is increased and ω and ψ are decreased.

During flattening at a smooth surface, the splat thickness decreases when β increases and ω decreases. An increase in the solid volume fraction φ and a decrease in ψ cause an increase in ζ. The splat radius decreases when ω and φ are increased. A decrease in ψ leads to a decrease in ξ. The absolute value of $d\zeta/d\theta$ depends weakly on the variations in the spraying parameters. The value of $d\xi/d\theta$ enhances with an increase in β and decreases with an increase in φ and ω.

The final splat thickness decreases when *Re* increases. For the rough surface, the value of ζ_f increases with an increase in φ and ω, and with a decrease in ψ. The final splat radius decreases when φ and ω are increased. The value of ξ_f enhances when χ and ψ are increased. The behavior of the final splat thickness and radius is similar for the smooth surface.

Theoretical results obtained for the final splat thickness agree well with the experimental data. Analytical formulas to the final parameters of the flattening process can be used for engineering estimates.

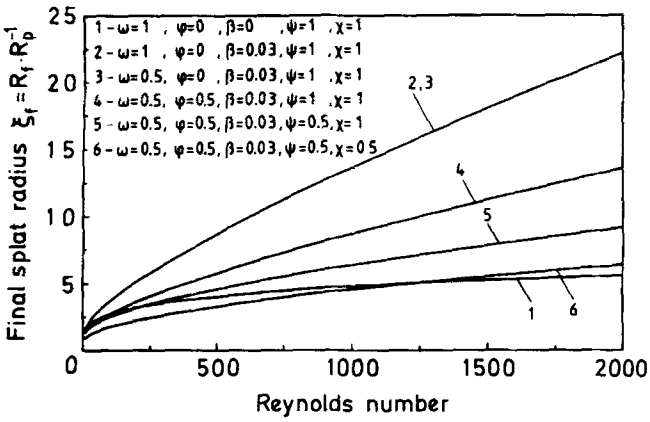

Fig. 10 Variation of final splat radius with Reynolds number for the smooth surface

Acknowledgments

The authors thank the Generalitat de Catalunya (GC) (project GRQ93-1017) and CICYT (project MAT96-0013) for financial support. Prof. V.V. Sobolev is grateful to GC for his visiting professor grant.

References

1. L. Pawlowski, *Science and Engineering of Thermal Spray Coatings*, John Wiley & Sons, 1994, p 327-360
2. R.C. Dykhuizen, Review of Impact and Solidification of Molten Thermal Spray Droplets, *J. Therm. Spray Technol.*, Vol 3 (No. 4), 1994, p 351-361
3. M. Vardelle, A. Vardelle, A.C. Leger, P. Fauchais, and D. Gobin, Influence of Particle Parameters at Impact on Splat Formation and Solidification in Plasma Spraying Processes, *J. Therm. Spray Technol.*, Vol 4 (No. 1), 1995, p 50-58
4. M. Bertagnolli, M. Marchese, and G. Jacucci, Modeling of Particles Impacting on a Rigid Substrate under Plasma Spraying Conditions, *J. Therm. Spray Technol.*, Vol 4 (No. 1), 1995, p 41-49
5. V.V. Sobolev and J.M. Guilemany, Flattening of Thermally Sprayed Particles, *Mater. Lett.*, Vol 22, 1995, p 209-213
6. V.V. Sobolev, J.M. Guilemany, and A.J. Martín, Influence of Surface Roughness on the Flattening of Powder Particles during Thermal Spraying, *J. Therm. Spray Technol.*, Vol 5 (No. 2), 1996, p 207-214
7. V.V Sobolev and J.M. Guilemany, Dynamic Processes during High Velocity Oxyfuel Spraying, *Int. Mater. Rev.*, Vol 41 (No. 1), 1996, p 13-32

8. V.V. Sobolev and J.M. Guilemany, Influence of Solidification on the Flattening of Droplets during Thermal Spraying, *Mater. Lett.*, Vol 28, 1996, p 71-75
9. V.V. Sobolev, J.M. Guilemany, and A.J. Martín, Investigation of Droplet Flattening during Thermal Spraying, *Surf. Coat. Technol.*, Vol 89, 1997, p 82-89
10. V.V. Sobolev, J.M. Guilemany, and J.A. Calero, Substrate-Coating Thermal Interaction during High Velocity Oxy-Fuel (HVOF) Spraying, Part 1: Heat Transfer Processes, *Mater. Sci. Technol.*, Vol 11 (No. 8), 1995, p 810-819
11. V.V. Sobolev, J.M. Guilemany, and J.A. Calero, Substrate-Coating Thermal Interaction during High Velocity Oxy-Fuel (HVOF) Spraying, Part 2: Structure Formation, *Mater. Sci. Technol.*, Vol 11 (No. 10), 1995, 1052-1059
12. V.V. Sobolev, J.M. Guilemany, J.A. Calero, and F.J. Villuendas, Heat Transfer between WC-Co Coating and Aluminum Alloy Substrate during High Velocity Oxygen-Fuel (HVOF) Spraying, *J. Therm. Spray Technol.*, Vol 4 (No. 4), 1995, p 408-414
13. V.V. Sobolev, J.M. Guilemany, and J.A. Calero, Formation of Structure of WC-Co Coatings on Aluminum Alloy Substrate during High Velocity Oxygen-Fuel (HVOF) Spraying, *J. Therm. Spray Technol.*, Vol 4 (No. 4), 1995, p 401-407
14. R.G. Boothroyd, *Flowing Gas-Solids Suspensions*, Chapman and Hall Ltd., London, 1971, p 8-43
15. S.L. Soo, *Fluid Dynamics of Multiphase Systems*, Blaisdell Publishing, 1967, p 133-276
16. V.V. Sobolev and P.M. Trefilov, *Thermophysics of Metal Solidification during Continuous Casting*, Metallurgy, Moscow, 1988, p 25-65
17. V.V. Sobolev, J.M. Guilemany, and J.A. Calero, Dynamic Processes during In-Flight Motion of Cr_3C_2-NiCr Powder Particles in High Velocity Oxy-Fuel (HVOF) Spraying, *J. Mater. Process. Manuf. Sci.*, Vol 4 (No. 1), 1995, p 25-39
18. C. Moreau, P. Cielo, and M. Lamontagne, Flattening and Solidification of Thermally Sprayed Particles, *J. Therm. Spray Technol.*, Vol 1, 1992, p 317-323
19. C.J. Li, A. Ohmori, and Y. Harada, Effect of WC Particle Size on the Formation of HVOF Sprayed WC-Co Coatings, *Thermal Spraying—Current Status and Future Trends*, High Temperature Society of Japan, Osaka, 1995, p 235-240